Static conformation and dynamics of single DNA molecules confined in nanoslits

Po-Keng Lin,[1] Chi-Cheng Fu,[2] Y.-L. Chen,[3,4,*] Yan-Ru Chen,[5] Pei-Kuen Wei,[4] C. H. Kuan,[5] and W. S. Fann[1,2,6,†]
[1]*Department of Physics, National Taiwan University, Taipei 10617, Taiwan, Republic of China*
[2]*Institute of Atomic and Molecular Science, Academia Sinica, Taipei 10617, Taiwan, Republic of China*
[3]*Institute of Physics, Academia Sinica, Taipei, 11529 Taiwan, Republic of China*
[4]*Research Center for Applied Sciences, Academia Sinica, Taipei 11529, Taiwan, Republic of China*
[5]*Graduate Institute of Electronics Engineering and Department of Electrical Engineering, National Taiwan University, Taipei 10617, Taiwan, Republic of China*
[6]*Institute of Polymer Science and Engineering, National Taiwan University, Taipei 10617, Taiwan, Republic of China*
(Received 12 September 2006; revised manuscript received 30 March 2007; published 23 July 2007)

Nearly thirty years ago, Daoud and de Gennes derived the scaling predictions for the linear polymer chains trapped in a slit with dimension close to the Kuhn length; however, these predictions have yet to be compared with experiments. We have fabricated nanoslits with vertical dimension similar to the Kuhn length of ds-DNA (110 nm) using standard photolithography techniques. Fluorescently labeled single DNA molecules with contour lengths L ranging from 4 to 75 μm were successfully injected into the slits and the chain molecules undergoing Brownian motions were imaged by fluorescence microscopy. The distributions of the chain radius of gyration and the two-dimensional asphericity were measured. It is found that the DNA molecules exhibit highly anisotropic shape and the mean asphericity is chain length independence. The shape anisotropy of DNA in our measurements is between two and three dimensions (2D and 3D). The static scaling law of the chain extension and the radius of gyration $\langle R_{\|}\rangle, \langle R_g\rangle \sim L^{\nu}$ were observed with $\nu_{R\|}=0.65\pm0.02$ and $\nu_{\mathrm{Rg}}=0.68\pm0.05$. These results are close to the average value between two ($\nu_{R\|,\mathrm{Rg}}=0.75$) and three ($\nu_{R\|,\mathrm{Rg}}=0.6$) -dimensional theoretical value. The scaling of the extensional and rotational relaxation time are between Rouse model in nanoslits and Zimm model in the bulk solution, respectively. We show that the conformation and chain relaxation of DNA confined in a slit close to Kuhn length exhibit the quasi-two-dimensional behavior.

DOI: 10.1103/PhysRevE.76.011806 PACS number(s): 61.25.Hq, 47.57.Ng

I. INTRODUCTION

Micro- or nanofabrication is a powerful tool to build up the nanofluidic device that cannot only manipulate and analyze single DNA molecules [1–3], but also provide a precise control of the geometry to test the physics of polymer in confined environments [4–7]. Understanding the conformation and dynamics of polymers in two-dimensional systems is an important problem that has applications related to protein-membrane interactions [8,9] as well as polymer adsorption on surfaces [10–13]. The contour length of a fluorescently labeled genomic DNA can be more than a micron and imaged under the fluorescent optical microscope. In the last decade, the conformation and dynamics of DNA molecules have been extensively studied at the single-molecule level in bulk solution [14,15], parallel-plate slit microchannel confinement [16–18], and slitlike nanochannels [19,20].

A polymer confined in a narrow parallel slit channel can be considered as a chain of spherical blobs [21] as the width of the slit becomes much smaller than its radius of gyration. The diameter of a blob is defined by the height of the slit channel h. Within each blob, the chain segments are assumed to have the same structure and dynamics as in a bulk solution and obey the three-dimensional (3D) self-avoiding walks. On the length scale larger than h, the polymer can be treated as a chain of 2D self-avoiding blobs with $n=N/g$ blobs, where N is the number of monomers of the polymer (i.e., the number of base pairs of DNA) and g is the number of monomers in a blob. In a truly two-dimensional system such as DNA adsorbed on a membrane, the blobs exclude each other and the excluded area of each blob is πh^2. In the case of parallel slit channels, the polymers are not adsorbed onto the surface, and the additional degree of freedom allows the polymers to exhibit quasi-2D behavior.

The shape of a long flexible polymer chain containing n Kuhn segments is in the same universality class as an n-step random walk. On a time scale longer than the rotational time of the polymer, the flexible polymer appears to have spherical symmetry through averaging over many conformations and orientations. However, the instantaneous chain conformation is highly anisotropic even for random walks, as first presented by Kuhn [22]. The shape of the random walks was determined using exact analytical calculations [23,24], $1/d$ expansions [25], and computer simulations [26]. The shape of random walks in two dimensions including self-avoiding effects was also discussed using simulations and theory [27–31]. The excluded volume interaction between polymer segments is stronger in two dimensions than in three dimensions. This is evident in the higher theoretical scaling exponent $R_g \sim n^{0.75}$ for two dimensions, as compared to $\sim n^{0.6}$ in three dimensions. On the experimental side, Haber *et al.* [32] investigated the shape of fluorescently labeled DNA molecules in bulk solution, and Maier *et al.* studied λ-DNA molecules adsorbed on membranes [12]. These works characterized the shape of flexible polymer in two and three dimensions as highly anisotropic.

*yenglong@phys.sinica.edu.tw
†fann@gate.sinica.edu.tw

More recently, Balducci *et al.* have measured the diffusivity of DNA in structures ranging from three dimensions to quasi-two dimensions [19]. They found the diffusivity scales inversely with the chain length, but the diffusivity scales with channel height differently than the blob scaling predictions. To our knowledge, our experiment is the first to investigate the polymer asphericity, conformation, and relaxation in the quasi-2D confinement. Our results provide deeper understanding for the manipulation of single DNA molecules in a nanofluidic device. In this paper, the chain shape, the chain diffusivity, the chain extension, and the relaxation of individual fluorescently labeled ds-DNA were studied in the nanoslit geometry with channel height approximately equal to the Kuhn length which is a crucial length scale of confined polymer physics.

II. BLOB THEORY OF POLYMER CONFINED IN SLIT

The scaling analysis of the static properties of polymer trapped in narrow slit was first treated by Daoud and de Gennes [21] and subsequently by simulation [33]. The Flory radius of self-avoiding polymer in three dimensions [34] is $R_F=2pn^{3/5}$, where p is the persistence length of polymer. Schaefer generalized the Flory theory to self-flexible polymers [6,35]. The Flory radius becomes $R_F=(\pi pw/4)^{1/5}L^{3/5}$, where w is the width of ds-DNA, the contour length $L=Na$ and a is the monomer bond length [6,35]. This relation can be used to estimate the average chain extension $R_\parallel$ in the axis parallel to the slit walls for good solvent. Consider the entropic elasticity of the polymer and the excluded volume repulsion between the blobs. The free energy of polymer confined in a narrow parallel slit is given by

$$\frac{F(R_\parallel)}{k_BT}=\pi h^2\frac{(N/g)^2}{R_\parallel^2}+\frac{R_\parallel^2}{(N/g)h^2}. \tag{1}$$

Minimizing the free energy leads to the extension $R_\parallel$ of polymer trapped in the narrow parallel slit

$$R_\parallel\approx\sqrt{\pi}h\left(\frac{N}{g}\right)^{3/4}=\left(\frac{\pi^3pw}{4h}\right)^{1/4}L^{3/4}. \tag{2}$$

The dynamical scaling properties of polymer confined in a narrow slit has been investigated by theory [36] and simulations [37]. In the theoretical model [36], the hydrodynamic interactions (HI) between segments is strongly screened with exponential spatial decay, and HI is considered only between the segments within a blob but not between the blobs. Thus the drag behavior of blobs is like impenetrable spheres and the friction coefficient of a blob is $\xi_{blob}=6\pi\eta h$. The friction coefficient of the whole chain confined in the slit is $\xi_{chain}=(N/g)\xi_{blob}$, which leads to the diffusivity $D_{CM}=k_BT/\xi_{chain}\sim 1/N$, the same dependence as predicted by the Rouse model. To understand the extensional relaxation process confined in the slit, we consider the following: The chain extension exhibits the thermal fluctuations $\delta R_\parallel$, the elastic restoring force opposes chain extension. Therefore the polymer behaves like a spring in which the elastic free energy is $\delta F=k_BT\,(\delta R_\parallel^2/R_\parallel^2)$. Differentiating twice with respect to $\delta R_\parallel$, we then obtain the effective spring constant $k=k_BT/R_\parallel^2\sim(h/p)^{1/2}L^{-3/2}$. Balancing the elastic force and friction force of the whole chain leads to the extensional relaxation time [38]

$$\tau_\parallel\sim\frac{\xi_{chain}}{k}\sim\left(\frac{1}{h}\right)^{7/6}L^{5/2} \tag{3}$$

III. EXPERIMENTAL METHODS

A. Fabrication of device

The nanoslits were fabricated by using standard photolithography on silicon wafers to define the patterns and etched by inductive reactive ions etch (RIE) using a combination of CF_4 and O_2 gas. Subsequently, the chips were bonded with the 170-μm-thick Pyrex 7740 cover glass by anodic bonding method (temperature: ~300 °C, voltage: 700–1000 V). The nanoslits used in this experiment are 100 μm wide and 110 nm high. The vertical image of the sealed nanoslit is shown in Fig. 1(a).

B. Sample preparation

DNA molecules of four different lengths were used in these studies: F2 (N=9.42 kbps, Purigo Biotech), F1 (N=23.13 kbps, Purigo Biotech), λ (N=48.50 kbps, New England BioLabs), and T4 (N=165.02 kbps, Wako). The DNA molecules were dissolved in 1/2 TBE buffer with 10 mM NaCl and labeled with the fluorescent dye TOTO-1 (Molecular Probes) at a ratio of four base pairs per dye. The dye molecules are known to intercalate and distort the local structure of DNA and the salt concentrations also strongly affect the DNA stiffness, extending the contour length L and persistence length p to ~1.35 times of the DNA natural length. For example, the contour length and persistence length of λ-DNA are L=22.3 μm and p=67.5 nm after labeling [39–41]. For single molecule imaging, the DNA solution is further diluted to 2 μg/ml–20 ng/ml, depending on the lengths. The image buffer contains 0.1% pop-6 (v/v) (Applied Biosystems), 3% 2-mercaptoethanol (v/v) (Sigma-Aldrich), 0.1% β-D-glucose (w/w) (Sigma-Aldrich), 10 μg/ml catalase (Roche), and 50 μg/ml glucose oxidase (Roche) in 1/2 TBE buffer with 10 mM NaCl. The viscosity η of the image buffer is 1.09 cP at 293 K. In the buffer solution used here, the electrostatic interactions between segments within the DNA molecule are screened by monovalent salt ions (Na^+) at length scales larger than the Debye screen length λ_D, which is approximately 3 nm (λ_D=0.3 nm/[NaCl]$^{1/2}$) [42]. Since this electrostatic screen length is much shorter than the excluded volume length $\nu^{1/3}$ of ds-DNA in a 110-nm slit, where $\nu=\pi p^2w$ is the excluded volume per rod and w is ~$2\lambda_D$ [19,43], the long range electrostatic interaction between segments can be neglected. The DNA in the current experiments can be considered to be fully neutral.

C. Fluorescence microscopy and image analysis

DNA solution was loaded into the nanoslit chips using capillary flow; usually the Brownian motion of DNA mol-

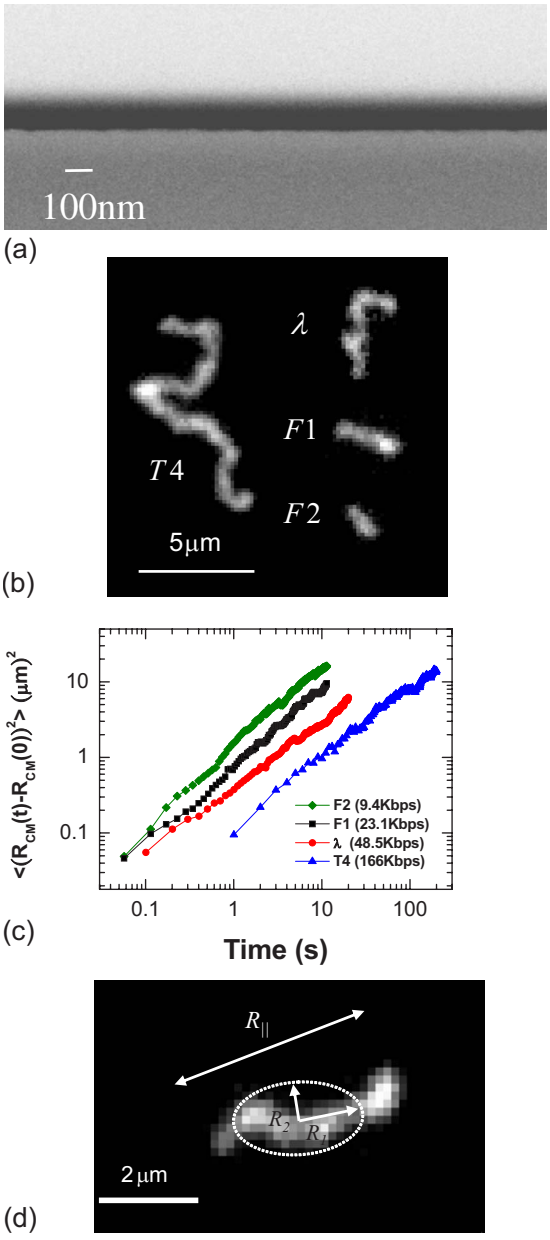

FIG. 1. (Color online) (a) Cross-sectional scanning electron image of the 110-nm slit. (b) The fluorescence image of T4-DNA, λ-DNA, F1-DNA, and F2-DNA, confined in the 110-nm slit. (c) The mean-squared displacements of center of mass vs time in double-logarithmic plot. (d) The λ-DNA image can be represented by an ellipse using the radius of gyration tensor, where R_1 is the major radius gyration component, R_2 is the minor radius gyration component, and $R_{\|}$ is the extension of this DNA image.

ecules can be observed after 30–60-min incubation. To avoid the interaction between DNA and the edge wall of the nanoslits, the microscope was focused away from the entrance and the exit of nanoslits (~30 μm). All experiments were performed at room temperature (~20 °C). TOTO-1 dyes labeled DNA molecules were excited with an argon laser at 514 nm (Coherent Innova 90) and monitored using an Olympus IX70 microscope with a 100× (NA 1.35, resolution 0.4 μm) oil immersed objective. Typically, the wide-field fluorescence images were taken by an electromagnetic charge-coupled device (CCD) (Andor DV887DCS-BV) with 0.01-, 0.033-, and 0.1-s exposure time. As discussed later, the rotational relaxation time of the DNA molecules are much slower than the exposure time, thus the images were captured without rotational averaging. Generally, 200 frames over a period of 11–200 s were recorded for each DNA molecule. The longer observation times correspond to longer DNA relaxation times. We synchronize the shutter to our CCD to get evenly fluorescent images of DNA and prevent the photoblanching of the DNA image. Figure 1(b) shows the fluorescent images of the DNA molecules in the nanoslit.

The total density of a single DNA molecule, $I(t)$, can be calculated from the intensity distribution function $I(\mathbf{r},t)$ with a set of coordinates $\mathbf{r}$. After subtracting the background intensity, the zeroth moment

$$I(t) = \int I(\mathbf{r},t)d\mathbf{r} \tag{4}$$

accounts for the total intensity $I(t)$ of a single DNA molecule. The information of $I(t)$ and its decay as a function of time allows us to quantify the fluorescent bleaching effect, which is corrected for in our analysis. The molecular center of mass is given by

$$\mathbf{R}_{CM}(t) = \frac{1}{I(t)} \int \mathbf{r}I(\mathbf{r},t)d\mathbf{r}. \tag{5}$$

The diffusivity of the DNA chain, D_{CM}, is determined from the mean-square displacement with time

$$\langle[\mathbf{R}_{\mathrm{CM}}(t) - \mathbf{R}_{\mathrm{CM}}(0)]^2\rangle = 4D_{\mathrm{CM}}t. \tag{6}$$

Figure 1(c) shows the mean-square displacement of center of mass as a function of time. The mean-square displacement of the DNA molecules increases linearly with time, as expected.

The shape and size of the DNA molecule are defined by calculating the radius of gyration tensor, given by

$$\mathbf{M}_{i,j}(t) = \frac{1}{I(t)} \int (\mathbf{r}_i - \mathbf{R}_{\mathrm{CM},i})(\mathbf{r}_j - \mathbf{R}_{\mathrm{CM},j})I(\mathbf{r},t)d\mathbf{r}, \tag{7}$$

where $I(\mathbf{r})$ is the fluorescence intensity of a pixel at positions $\mathbf{r}$. From the DNA images, which are two dimensional, the major and minor eigenvalues of $\mathbf{M}_{i,j}$, R_1^2, and R_2^2, are calculated. Figure 1(d) shows R_1 and R_2 as the characteristic lengths of the major and minor axis in the DNA image, respectively. The size and shape are quantified by the square radius of gyration $R_g^2 = R_1^2 + R_2^2$ and the asphericity $A_2 = (R_1^2 - R_2^2)^2/(R_1^2 + R_2^2)^2$ [23,24]. The mean asphericity $\langle A_2 \rangle$ is defined as $\langle (R_1^2 - R_2^2)^2 \rangle / \langle (R_1^2 + R_2^2)^2 \rangle$. The value of $\langle A_2 \rangle$ can range from 0 to 1, where the extreme values correspond to the spherically symmetric shape ($\langle A_2 \rangle = 0$) and the rodlike shape ($\langle A_2 \rangle = 1$).

IV. RESULTS AND DISCUSSION

A. Shape of DNA in quasi-2D nanoslit

Figure 2(a) shows the probability distribution of R_1^2 and R_2^2 for the λ-DNA. The distribution functions appear to be

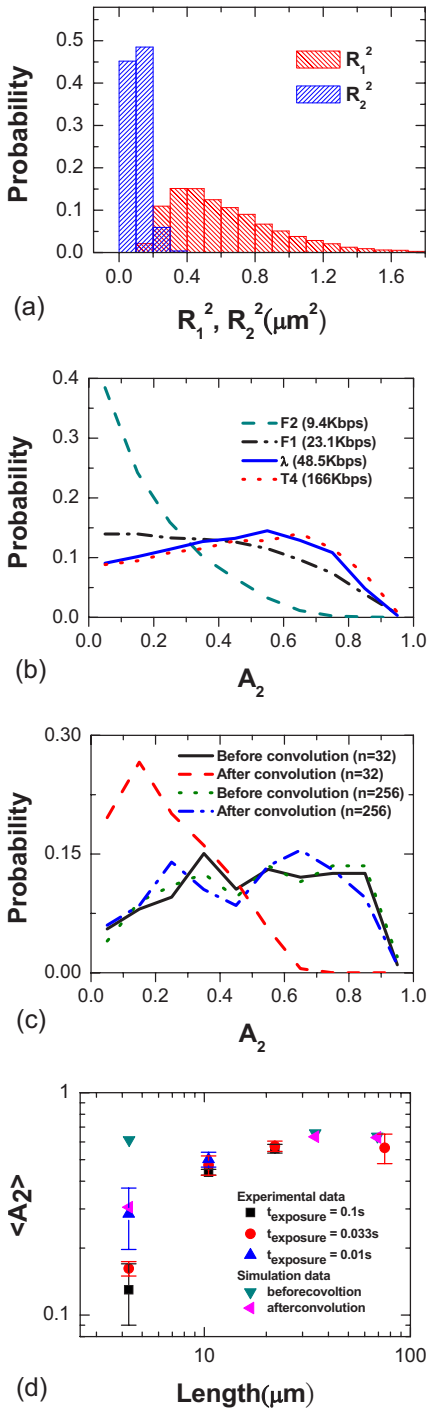

FIG. 2. (Color online) (a) The probability distributions of R_1^2 and R_2^2 for λ-DNA; the mean values of the major and minor eigenvalues are $\langle R_1^2\rangle = 0.62 \pm 0.33\ \mu m^2$ and $\langle R_2^2\rangle = 0.12 \pm 0.05\ \mu m^2$, respectively. (b) The probability distribution of experimental measurements for the asphericity A_2. The exposure time of F2–F1 and λ–T4 are 0.01 and 0.033 s, respectively. (c) The probability distribution of the simulation results for A_2 with chain length $n=32$ (solid: before convolution; dashed: after convolution) and $n=256$ (dotted: before convolution; dash-dotted: after convolution). (d) The mean asphericity $\langle A_2\rangle$ with different chain lengths with different $t_{exposure}$ for experiment (F2–T4) and simulation ($n=32$, 256, and 512). The error bars represent the standard deviation calculated from the distribution of measured single molecule mean asphericity.

TABLE I. The shape properties of DNA can be compared to the Monte Carlo simulation of 2D nonexcluded volume chains (NEV) and excluded volume chains (EV) with the $n=32$ chain [29].

N (kbp)	$\langle R_g^2\rangle$	$\langle R_1^2\rangle/\langle R_g^2\rangle$	$\langle R_2^2\rangle/\langle R_g^2\rangle$	$\langle A_2\rangle$
9.42 (F2)	0.09±0.03	0.65±0.26	0.35±0.14	0.29±0.10
23.13 (F1)	0.26±0.11	0.81±0.42	0.19±0.08	0.50±0.04
48.50 (λ)	0.74±0.32	0.84±0.45	0.15±0.07	0.56±0.03
165.02 (T4)	3.59±1.44	0.84±0.41	0.15±0.08	0.57±0.09
$n=32$ (NEV)		0.84	0.16	0.60±0.10
$n=32$ (EV)		0.87	0.13	0.62±0.02

asymmetric Gaussian functions, and the distribution of R_1^2 has a larger mean and width than the distribution of R_2^2, which suggests the DNA molecules have highly anisotropic shapes. Figure 2(b) shows the probability distribution of the asphericity with different chain lengths. For the shortest chain (F2), the chain shape appears mostly spherical. For the longer chains, the distribution is very broad and even. The mean asphericity for several DNA molecules is presented in Table I. The normalized major eigenvalues $\langle R_1^2\rangle/\langle R_g^2\rangle$ increases with increasing L, while the normalized minor eigenvalue $\langle R_2^2\rangle/\langle R_g^2\rangle$ decreases with increasing L. The ratio $\langle R_1^2\rangle/\langle R_2^2\rangle$ thus increases with increasing L. Our experimental results can be compared to previous experiment of λ-DNA adsorbed on fluid lipid membranes by Maier and Rädler in a truly 2D system [12]. Their experiments found $\langle R_1^2\rangle/\langle R_2^2\rangle = 6$, $\langle A_2\rangle = 0.61$, $\langle R_1^2\rangle/\langle R_g^2\rangle = 0.84$, $\langle R_2^2\rangle/\langle R_g^2\rangle = 0.14$, and $\langle R_g^2\rangle = 3.2 \pm 0.3\ \mu m^2$. The size and shape of λ-DNA of their results are larger and more anisotropic than our measurements of $\langle R_g^2\rangle = 0.74 \pm 0.32\ \mu m^2$ and $\langle A_2\rangle = 0.56 \pm 0.03$. These differences can be attributed to the differences of the 2D fluid membrane and the quasi-2D nanoslit. Experimentally, Haber *et al.* [32] used the ensemble-averaged $\langle R_1/R_2\rangle$ (the ratio between the major axis and the minor axis) to describe the shape anisotropy of T2 DNA in bulk solution. They found $\langle R_1/R_2\rangle = 2.20$, for our result of T4 DNA $\langle R_1/R_2\rangle = 2.57$, which suggests the quasi-2D confined DNA is less spherical than in bulk solution.

Previous theory and simulations have suggested that the shape of a confined DNA molecule does not depend strongly on its molecular weight, thus the observation that the short DNA is more spherical than the long DNA needs to be addressed. The lateral resolution of the DNA image is limited by the instrument response of the microscope. The measured fluorescence intensity distribution can be treated as the true image of dyes on the DNA backbone convoluted with the point spread function (PSF) of the optical system. This blurring effect causes the apparent size of the fluorescent DNA molecules to be larger than the actual size, and the effect will be more pronounced for the shorter chain [44]. To quantify this bias on the shape of DNA, we measure the intensity profile of 40-nm fluorescent spheres (the size is close to p) confined in the 110-nm slit to obtain the PSF of the optical system and the measured PSF did not depend on exposure time (0.01–0.033 s). The simulation results are convoluted with the PSF and compared with the experiments. In previ-

ous simulations of self-avoiding walks, the asphericity varies little from $n=16$ to 40 000 [29,31]. Similar chain-length independence is also found in simulation studies of an ideal random-walk chain [30]. For comparison with the experiments, the Monte Carlo (MC) simulation of the self-avoiding random walks with n segments and the segment length l corresponds to the Kuhn length of the DNA molecule.

For simplicity, DNA is represented as a bead-spring chain, where the nonbonded beads repel each other with a cutoff-shifted Lennard-Jones potential given by

$$\frac{U_{LJ}(\mathbf{r})}{k_BT}=\begin{cases}4\dfrac{\varepsilon}{k_BT}\left[\left(\dfrac{\sigma}{\mathbf{r}}\right)^{12}-\left(\dfrac{\sigma}{\mathbf{r}}\right)^{6}\right]-U_{LJ}(\mathbf{r}=\mathbf{R}_{cut}) & \mathbf{r}<\mathbf{R}_{cut}\\ 0 & \mathbf{r}>\mathbf{R}_{cut}\end{cases}, \tag{8}$$

where r denotes the distance between the beads, σ is the bead diameter, $\varepsilon/k_BT=0.2$, and $R_{cut}=2.5\sigma$ denotes the cutoff radius. The bonded beads are connected with a harmonic potential $U_{bond}/(k_BT)=k_v/2\ (|\mathbf{r}_i-\mathbf{r}_{i-1}|-l)^2$ with $k_v=400$ and the equilibrium length $l=1\sigma$ [45]. This polymer model has the scaling exponent of a self-avoiding walk. The off-lattice simulation method employed monomer displacement, reptation, and configurational-biased Monte Carlo moves [45] to sample the energy landscape of the polymer. The chain is confined in a slit of height $H=2\sigma$. For statistical sampling, 200 independent configurations are selected from configurations with no correlations in R_g.

Figure 2(c) shows the simulation data for $n=32$ chain and $n=256$ chain with and without convolution. Under the experimental conditions, the Kuhn length is approximately 135 nm and the $n=32$ model chain corresponds to 4.3 μm, which is close to the contour length of F2, $n=256$ corresponds to 34.6 μm (between λ-phage and T4) and $n=512$ corresponds to 69.1 μm which is close to the contour length of T4. The probability distributions of A_2 for the $n=32$ chain becomes narrower after the convolution. The A_2 distribution of $n=32$ shifts to the spherical region. In contrast, the A_2 distribution of $n=256$ changes only slightly. Figure 2(d) shows the mean asphericity $\langle A_2\rangle$ for experimental and simulation data for different chain lengths with different exposure time $t_{exposure}$. We find the $\langle A_2\rangle$ is approximately 0.6 for every chain length in the simulations. When the simulated chain configurations are convoluted with the PSF, $\langle A_2\rangle$ is found to decrease with decreasing chain length (F1–T4). This is consistent with our experimental observations, where the results suggest the $\langle A_2\rangle$ of not too short DNA molecules (F1–T4) is chain length independence. For the shortest chain (F2), the $\langle A_2\rangle$ is a strong decrease with increasing $t_{exposure}$. The blurring effect from the size asymmetry change in one exposure time is caused by the fast motion of F2 and its size is too short.

For the continuous chains, analytic calculation of the mean asphericity in d-dimensional random walks finds $\langle A_2\rangle=(2d+4)/(5d+4)$ [23,24] and $\langle A_2\rangle=0.571$. Aronovitz and Nelson used first-order $\varepsilon=4-d$ expansion to calculate $\langle A_d\rangle$ for continuous self-avoiding walks, and they found $\langle A_2\rangle=(2d+4)/(5d+4)+0.008\varepsilon$ [23], where $\langle A_2\rangle=0.587$. The change in the chain shape between ideal and self-avoiding random walks is very small. Within the experimental error, both calculations are consistent with the current measurements. The experimental and simulation study in our work suggests that the A_2 is chain length independent.

B. Static scaling analysis of DNA in quasi-2D nanoslit

According to Flory's theory (mean-field calculations) [34], the average radius of gyration ($\langle R_g\rangle$) of a chain molecule should scale as $\langle R_g\rangle\sim N^{\nu_d}$, where ν_d is the Flory exponent depending on the dimension of environment d. In good solvent conditions, $\nu_d=3/(d+2)$, which gives $\nu_d=0.75$ and 0.6 for $d=2,3$, respectively. Daoud and de Gennes also predicted that the polymer confined in parallel slit can be treated as a 2D self-avoiding blob chain with the segment length about h. In our experiments, h is close to the Kuhn length of DNA and a length scale regime suited for testing the blob theory. The $\langle R_g\rangle$ and $\langle R_\parallel\rangle$ of the DNA are calculated by averaging uncorrelated DNA conformations, determined by calculating the autocorrelation functions $\langle R_g(0)R_g(t)\rangle$ and $\langle R_\parallel(0)R_\parallel(t)\rangle$. Figure 3(a) shows $\langle R_g\rangle$ and $\langle R_\parallel\rangle$ as a function of N, the scaling exponent $\nu_{Rg}=0.68\pm0.05$ and $\nu_\parallel=0.65\pm0.02$, which are between the prediction of self-avoiding walks in two dimensions ($\nu=0.75$) and three dimensions ($\nu=0.6$). [27–29]. The observed scaling exponents suggest that the DNA molecules confined in the 110-nm slit do not have 2D scaling, but the scaling is between two and three dimensions, or quasi-two dimensions. Table II shows the results of $\langle R_g\rangle$ with different exposure time. The $\langle R_g\rangle$ of data ($t_{exposure}=0.033$ s) is smaller than the data ($t_{exposure}=0.1$ s). For the T4 DNA, the total observation times are 20 and 200 s for the data of $t_{exposure}=0.1$ s and $t_{exposure}=0.033$ s, respectively. In the data ($t_{exposure}=0.1$ s), the total observation time of 20 s is not much larger than the relaxation time (~5 s) of T4 DNA. The correlated sampling of DNA conformations is the main cause of differences of $\langle R_g\rangle$ and ν_{Rg} between data of $t_{exposure}=0.1$ s and $t_{exposure}=0.033$ s. According to Eq. (2), the mean extension of λ-DNA in the 110-nm slit should be 4.03 μm, using $w=5$ nm, $p=67.5$ nm, and $L=22.3$ μm. This value is slightly larger than the measured extension of 3.23 ± 0.64 μm.

Smith *et al.* [14] investigated the isolated linear DNA dynamics in bulk solution using fluorescence microscopy. They showed that the diffusivity of DNA in bulk solution (D_{bulk}) exhibits Zimm behavior. The R_g can be calculated from D_{bulk} base on the Zimm model $D_{bulk}=0.08k_BT/\eta R_g$ [14,46] with k_BT the thermal energy. For λ-DNA, the R_g in bulk solution is 0.73 μm. In the 2D system, the pioneering experiments of Maier and Rädler [10] found that R_g follows a power law scaling with N ($R_g\sim N^{0.79\pm0.04}$) and the $\langle R_g\rangle$ of λ-DNA is 1.9 μm. This value is much larger than our finding of λ-DNA in a nanoslit ($\langle R_g\rangle=0.84\pm0.18$ μm), which can be attributed to the stronger self-avoiding interactions within the DNA chain for the 2D system.

C. Dynamics scaling analysis of DNA in quasi-2D nanoslit

The diffusion coefficient D_{CM} was obtained by a linear fit of an ensemble average (typically ten molecules over

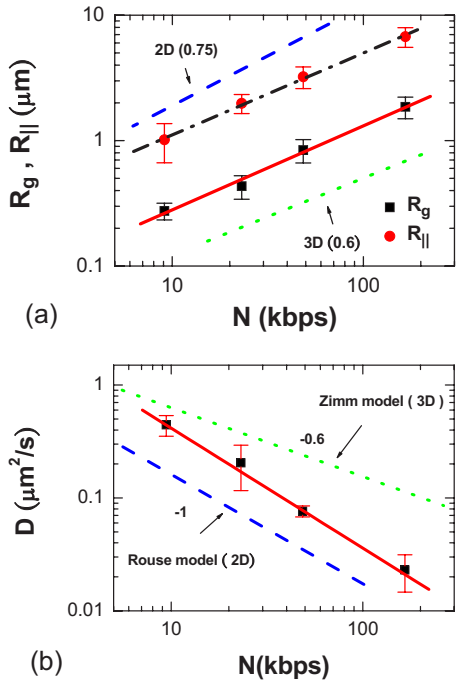

FIG. 3. (Color online) Static and dynamical scaling analysis of DNA confined in the 110-nm slit. All statistical quantities were calculated from 20–75 individual DNA molecules with exposure time (0.033 s). Linear fit to the data leads to the scaling exponent. (a) The radius of gyration ($\langle R_g \rangle$) and mean extensions ($\langle R_{||} \rangle$) vs the number of base pairs (N) for experimental results of the nanoslit. The dashed line and the dotted line are scaling theory predictions of the self-avoiding chain in two dimensions (0.75) and in three dimensions (0.6), respectively. The error bars represent the standard deviation of the distribution of $R_{||}$. The slopes of linear fitting for R_g (solid line) and $R_{||}$ (dash-dotted line) are 0.68±0.05 and 0.65±0.02, respectively. (b) Diffusivity (D_{CM}) vs number of base pairs (N) for experimental results of the nanoslit. The D_{CM} was determined by averaging the trajectories of ten DNA molecules over 10–50 s. The scaling exponent of D_{CM} is −1.05±0.05. The dashed line and the dotted line are the scaling predictions of the Rouse model in two dimensions and the Zimm model in three dimensions, respectively.

10–50 s) of the time-dependent mean-square displacement. The dependence of D_{CM} on the chain length is shown in Fig. 3(b) and the scaling exponent ν_{DCM}=−1.05±0.05. This value is in good agreement with Rouse dynamics. The diffusivity

TABLE II. $\langle R_g \rangle$ and ν_{Rg} for different exposure times. The sampling time for the T4 DNA is 20 s for $t_{exposure}$=0.1 s and 200 s for $t_{exposure}$=0.33 s. The sampling time for F2, F1, and λ DNA is 20 s for both exposure times.

N (kbp)	$\langle R_g \rangle$ $t_{exposure}$=0.1 s	$\langle R_g \rangle$ $t_{exposure}$=0.033 s
9.42 (F2)	0.30	0.28
23.13 (F1)	0.43	0.43
48.50 (λ)	0.91	0.84
165.02 (T4)	2.42	1.86
ν_{Rg}	0.75	0.68

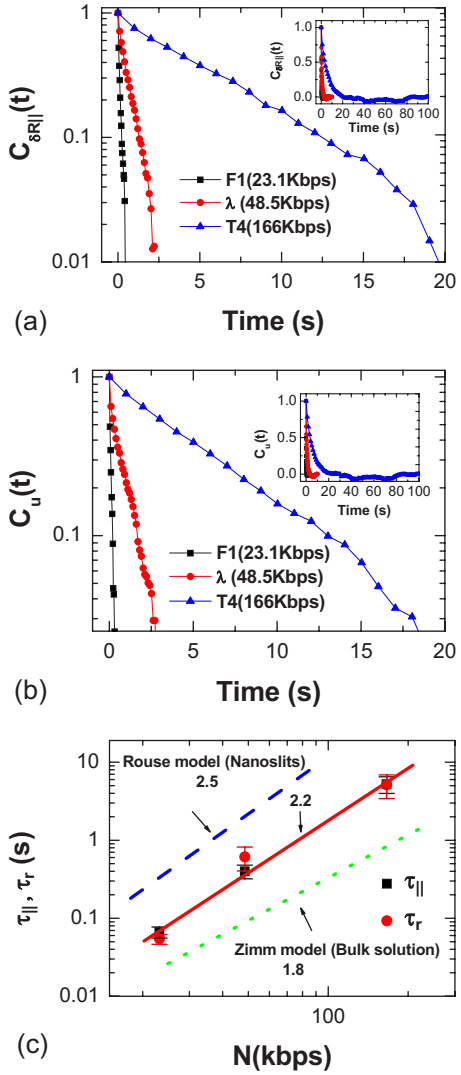

FIG. 4. (Color online) Extensional and rotational relaxation analysis of DNA molecules. (a) The autocorrelation function $C_{\delta R||}$ of extension fluctuation δR. (b) The time correlation function of $u(t)$. The $C_{\delta R||}$ and $C_u(t)$ show the single exponential decays and the insets in (a) and (b) show the linear plot of the autocorrelation function. (c) The data of $\tau_{||}$ and τ_r around the solid line (slope =2.2). The dashed line and dotted line show the theory scaling prediction of the Rouse model in nanoslits and the Zimm model in the bulk solution, respectively.

of our observation is much larger than the measurements on DNA bound to fluidic cationic lipid membranes [10,11]. In addition to the difference between two dimensions and quasi-two dimensions, there is one key difference for DNA in the membranes. The membrane surface is oil-like, and the viscosity is high. Recent work [19] investigated the DNA diffusivity in a nanoslit with changing the channel depth and the chain length. Our measurements of scaling exponent and diffusivity are in good agreement with their findings. The experimental results of D_{CM} can be compared with the measurements of DNA in bulk solution [14] and microchannel [18]. According to the Rouse scaling theory predictions, the normalized diffusivity (D_{CM}/D_{bulk}) scales with the inverse normalized channel width $(R_{g,bulk}/h)^{\nu}$ with exponent

$\nu_{DCM/D\text{bulk}}=-2/3$. The experimental data over a range $R_{g,\text{bulk}}/h=2.8-13.9$ and the scaling exponent $\nu_{D/D\text{bulk}}=-0.78\pm0.12$ is found, in agreement with recent simulations and Rouse dynamics.

The extensional relaxation time $\tau_\parallel$ and rotational relaxation time τ_r are the longest relaxation times for the internal motion of a polymer, and they are the characteristic times for sampling uncorrelated DNA conformations. Scaling theory predictions show that $\tau_r \sim N^{1.8}$ in the bulk solution (Zimm, good solvent) [46] and $\tau_r \sim N^{2.5}$ in the nanoslit (Rouse, good solvent) [38]. DNA molecules in bulk solution have a random coil configuration and it is difficult to directly observe the rapid Brownian fluctuations of DNA using fluorescence microscopy. Steve Chu's group found that the relaxation of near fully stretched DNA scales as $\tau_\parallel \sim N^{1.66}$ in the bulk solution [40], which is the scaling behavior predicted by the Zimm model prediction. For polymers confined in a slit, the extensional relaxation time $\tau_\parallel$ and rotational relaxation time τ_r were obtained by fitting the autocorrelation function of the $C_{\delta R\parallel}=\langle \delta R_\parallel(0)\delta R_\parallel(t)\rangle$ and $C_u=\langle u(0)u(t)\rangle$, respectively. $\delta R_\parallel(t)=R_\parallel(t)-\langle R_\parallel\rangle$ denotes the fluctuation of the extension, and the unit vector $u(t)$ is defined as the direction parallel to the major axis of the radius of gyration tensor R_1. Figures 4(a) and 4(b) show $C_{\delta R\parallel}$ and C_u, respectively. As shown in Fig. 4(c), the translational and rotational relaxation times depend on the chain length, and the measured scaling exponents for both are $\nu=2.2$. This value is between the Rouse model prediction for a chain in a 2D good solvent ($\nu_{\pi r}=2.5$) and the Zimm model prediction for a chain in three dimensions ($\nu_{\pi r}=1.8$), suggesting that hydrodynamic interactions are partially screened. Our observed rotational relaxation time τ_r for λ-DNA is 0.61 s, which is much smaller than that reported for DNA bound on the fluidic cationic lipid membrane [11], where $\tau_{r,\text{lipid}}\approx 1500$ s. For DNA molecules bound on the lipid membrane, the relaxation mechanism appears to be dominated by reptation [13], leading to much slower relaxation. Matsumoto *et al.* [16] studied the Brownian motion of T4 DNA confined in parallel-plate slit microchannels ($h=4$ μm, $R_{g,\text{bulk}}/h\approx 0.35$) and found $\tau_r\approx 3.5$ s, which is consistent with the Zimm model predictions for DNA in the bulk solution. As expected, the rotational relaxation time in the bulk is faster than the current observation of $\tau_r=5$ s for T4 DNA in a 110-nm nanoslit ($R_{g,\text{bulk}}/h\approx 13.9$).

V. CONCLUSION

We have systematically investigated the shape, the extension, and the dynamics of ds-DNA molecules in quasi-2D confinement of 110-nm slits. The experiments are performed over a sufficient time period longer than the rotational relaxation time of the longest polymer T4 DNA. Our experiments show that a sufficiently longer observation time than the DNA's longest relaxation time is required to ensure proper sampling of uncorrelated conformations. This is particularly important for DNA molecules confined to a length scale near or below its persistence length, where the chain relaxation process can slow down significantly. The chain diffusivity dependence on the chain length agrees well with the scaling prediction of the Rouse scaling, suggesting that hydrodynamic interactions are at least partially screened in this system [19]. The measured chain length dependence of the extensional relaxation time $\tau_\parallel$ and the rotational relaxation time τ_r are between the Rouse scaling for a 2D chain and Zimm scaling for a 3D chain. The discrepancies of the static scaling and relaxation are consistent with the experiments being performed in quasi-2D confinement rather than dimensions.

Our results for the static DNA conformations show that the scaling exponents of the extension $\langle R_\parallel\rangle$ and the radius of gyration $\langle R_g\rangle$ of quasi-2D confined DNA molecules are indeed between the scaling theory predictions for 2D and 3D polymer. Observations of the shape anisotropy of DNA accounting for the fluorescence smearing effect agree with the MC simulations. The mean asphericity is chain length independent. It is clear from our investigations that confinement on the DNA persistence length scale strongly affects its conformation. Our future work will investigate how changes to the DNA flexibility due to confinement affect its interactions with nanoparticles on the order of the DNA persistence length and smaller.

ACKNOWLEDGMENTS

This research was supported by the Academia Sinica and the National Science Council through the National Program for Nanoscience and Nanotechnology (Grant No. NSC 94-2120-M-002-009).

[1] Y. M. Wang, J. O. Tegenfeldt, W. Reisner, R. Riehn, X. J. Guan, L. Guo, I. Golding, E. C. Cox, J. Sturm, and R. H. Austin, Proc. Natl. Acad. Sci. U.S.A. **102**, 9796 (2005).
[2] R. Riehn, M. C. Lu, Y. M. Wang, S. F. Lim, E. C. Cox, and R. H. Austin, Proc. Natl. Acad. Sci. U.S.A. **102**, 10012 (2005).
[3] J. P. Fu, J. Yoo, and J. Y. Han, Phys. Rev. Lett. **97**, 018103 (2006).
[4] J. O. Tegenfeldt, C. Prinz, H. Cao, S. Chou, W. W. Reisner, R. Riehn, Y. M. Wang, E. C. Cox, J. C. Sturm, P. Silberzan, and R. H. Austin, Proc. Natl. Acad. Sci. U.S.A. **101**, 10979 (2004).
[5] W. Reisner, K. J. Morton, R. Riehn, Y. M. Wang, Z. N. Yu, M. Rosen, J. C. Sturm, S. Y. Chou, E. Frey, and R. H. Austin, Phys. Rev. Lett. **94**, 196101 (2005).
[6] C. H. Reccius, J. T. Mannion, J. D. Cross, and H. G. Craighead, Phys. Rev. Lett. **95**, 268101 (2005).
[7] J. T. Mannion, C. H. Reccius, J. D. Cross, and H. G. Craighead, Biophys. J. **90**, 4538 (2006).
[8] J. O. Radler, I. Koltover, T. Salditt, and C. R. Safinya, Science **275**, 810 (1997).
[9] T. Salditt, I. Koltover, J. O. Radler, and C. R. Safinya, Phys. Rev. Lett. **79**, 2582 (1997).
[10] B. Maier and J. O. Radler, Phys. Rev. Lett. **82**, 1911 (1999).

[11] B. Maier and J. O. Radler, Macromolecules **33**, 7185 (2000).
[12] B. Maier and J. O. Radler, Macromolecules **34**, 5723 (2001).
[13] S. A. Sukhishvili, Y. Chen, J. D. Muller, E. Gratton, K. S. Schweizer, and S. Granick, Nature (London) **406**, 146 (2000).
[14] D. E. Smith, T. T. Perkins, and S. Chu, Macromolecules **29**, 1372 (1996).
[15] R. M. Robertson, S. Laib, and D. E. Smith, Proc. Natl. Acad. Sci. U.S.A. **103**, 7310 (2006).
[16] M. Matsumoto, T. Sakaguchi, H. Kimura, M. Doi, K. Minagawa, Y. Matsuzawa, and K. Yoshikawa, J. Polym. Sci., Part B: Polym. Phys. **30**, 779 (1992).
[17] O. B. Bakajin, T. A. J. Duke, C. F. Chou, S. S. Chan, R. H. Austin, and E. C. Cox, Phys. Rev. Lett. **80**, 2737 (1998).
[18] Y. L. Chen, M. D. Graham, J. J. de Pablo, G. C. Randall, M. Gupta, and P. S. Doyle, Phys. Rev. E **70**, 060901(R) (2004).
[19] A. Balducci, P. Mao, J. Han, and P. S. Doyle, Macromolecules **39**, 6273 (2006).
[20] D. Stein, F. H. J. van der Heyden, W. J. A. Koopmans, and C. Dekker, Proc. Natl. Acad. Sci. U.S.A. **103**, 15853 (2006).
[21] M. Daoud and P. G. de Gennes, J. Phys. (Paris) **38**, 85 (1977).
[22] W. Kuhn, Kolloid-Z. **68**, 2 (1934).
[23] J. A. Aronovitz and D. R. Nelson, J. Phys. (Paris) **47**, 1445 (1986).
[24] J. Rudnick and G. Gaspari, Science **237**, 384 (1987).
[25] G. Gaspari, J. Rudnick, and A. Beldjenna, J. Phys. A **20**, 3393 (1987).
[26] S. J. Sciutto, J. Phys. A **27**, 7015 (1994).
[27] M. Bishop and J. P. J. Michels, J. Chem. Phys. **85**, 1074 (1986).
[28] M. Bishop and J. P. J. Michels, J. Chem. Phys. **83**, 4791 (1985).
[29] M. Bishop and C. J. Saltiel, J. Chem. Phys. **85**, 6728 (1986).
[30] S. J. Sciutto, J. Phys. A **28**, 3667 (1995).
[31] S. J. Sciutto, J. Phys. A **29**, 5455 (1996).
[32] C. Haber, S. A. Ruiz, and D. Wirtz, Proc. Natl. Acad. Sci. U.S.A. **97**, 10792 (2000).
[33] J. H. Vanvliet, M. C. Luyten, and G. Tenbrinke, Macromolecules **25**, 3802 (1992).
[34] P. J. Flory, *Principles of Polymer Chemistry* (Cornell University Press, Ithaca, NY, 1971).
[35] D. W. Schaefer, J. F. Joanny, and P. Pincus, Macromolecules **13**, 1280 (1980).
[36] F. Brochard and P. G. de Gennes, J. Chem. Phys. **67**, 52 (1977).
[37] A. Milchev and K. Binder, J. Phys. II **6**, 21 (1996).
[38] F. Brochard, J. Phys. (Paris) **38**, 1285 (1977).
[39] N. Makita, M. Ullner, and K. Yoshikawa, Macromolecules **39**, 6200 (2006).
[40] T. T. Perkins, S. R. Quake, D. E. Smith, and S. Chu, Science **264**, 822 (1994).
[41] C. G. Baumann, S. B. Smith, V. A. Bloomfield, and C. Bustamante, Proc. Natl. Acad. Sci. U.S.A. **94**, 6185 (1997).
[42] S. Cocco, J. F. Marko, R. Monasson, A. Sarkar, and J. Yan, Eur. Phys. J. E **10**, 249 (2003).
[43] J. F. Marko and E. D. Siggia, Macromolecules **28**, 8759 (1995).
[44] K. Yoshikawa, M. Takahashi, V. V. Vasilevskaya, and A. R. Khokhlov, Phys. Rev. Lett. **76**, 3029 (1996).
[45] D. Frenkel and B. Smit, *Understanding Molecular Simulations: From Algorithms to Applications* (Academic, San Diego, 2001).
[46] M. Doi and S. F. Edwards, *The Theory of Polymers Dynamics* (Oxford University Press, Oxford, 1986).